

Fabrication of TiO_2 / Ag / Ag_3PO_4 Heterostructured Nanorod Arrays on FTO for Enhanced Photoelectrochemical and Photocatalytic Performances

Wei Liang^{1, a*}, Shengling Lin^{2, b}, Chuanxiang Chen^{3, c} and Ankang Chen^{3, d}

¹⁻³ School of Environmental and Chemical Engineering, Jiangsu University of Science and Technology, Mengxi Road, Jingkou District, Zhenjiang, P.R.China

^allww660008@foxmail.com, ^blinshl5757@sina.com, ^ccxchen@just.edu.cn, ^d960486211@qq.com

Keywords: TiO_2 nanorod arrays, Photocatalyst, Photoelectrochemical, Heteronanostructure.

Abstract. This research explores the preparation of $\text{TiO}_2/\text{Ag}/\text{Ag}_3\text{PO}_4$ heterostructured nanorod arrays on transparent conductive FTO glass for the first time. The structures and morphologies of the products were characterized by using scanning electron microscopy (SEM) and X-ray diffraction (XRD). Moreover, their photoelectrochemical performances under visible light irradiation have been explored by electrochemical techniques. The photocurrent density of $\text{TiO}_2/\text{Ag}/\text{Ag}_3\text{PO}_4$ nanorod arrays could reach up to $2.60 \text{ mA}\cdot\text{cm}^{-2}$, which is much higher than that of pure TiO_2 nanorod arrays ($1.20 \text{ mA}\cdot\text{cm}^{-2}$). In addition, the efficiency of $\text{TiO}_2/\text{Ag}/\text{Ag}_3\text{PO}_4$ arrays in photocatalytic degradation of RhB reached 94.5% within 3 hours, but pure TiO_2 nanorod arrays was only 74.8%. Above results are of great significance for the practical use of the as-prepared nanorod arrays.

Introduction

TiO_2 nanorod arrays (TiO_2 NRAs) have attracted intense interest in scientific applications due to they have high mechanical stability, large specific surface area and unique shape with fewer interfacial grain boundaries.¹ Moreover, they could facilitate efficient charge transport to minimize the loss of charge carriers.² However, the wide direct band gap (3.2 eV) leading to a relatively low conversion efficiency^{3,4} and the high rate recombination of photo-generated electron-hole pairs greatly limited the practical applications of TiO_2 NRAs. To settle above issues, much effort has been focused on sensitizing TiO_2 with narrow band gap semiconductor to enhance their performance.

Ag_3PO_4 acting as a light-sensitive material sensitive to visible light could be used to improve the separation efficiency of the light-generated electrons and holes. However, Ag_3PO_4 is easy to decompose in practical applications if no sacrificial reagent is supplied due to its weakly stability. Teng's previous studies have shown that elemental Ag as an electron acceptor can not only enhance the charge separation, but also prevent the reductive decomposition of Ag_3PO_4 .⁵

Experimental Details

Preparation of the TiO_2 NRAs. The TiO_2 NRAs were synthesized via a modified hydrothermal method.⁶ Firstly, 5.2 mL TBOT was added in 30 mL anhydrous alcohol under stirring in ice water bath. Then an optimized amount of mixed solution containing 0.45 mL deionized water, 20 mL anhydrous alcohol and 1.5 mL acetic acid was dropped into the above solution. Then FTO glass was soaked in the sol for 20 min. After the soaking process, the substrate was heated in an oven at 100 °C for 30 min. Secondly, 1 mL TBOT was added to the mixture solvent containing 10 mL acetic acid, 5 mL hydrochloric acid and 15 mL deionized water, in which the mass concentration of hydrochloric acid was 36%. After stirring of 30 min, the mixture solution was transferred to a 25 mL Teflon-lined stainless steel autoclave. Then TiO_2 -coated FTO glass were placed at an angle against the wall of the Teflon-liner with the conducting side facing down to grow TiO_2 NRAs at 200 °C for 8 h in a muffle furnace. The achieved product was then removed from the solution and rinsed with deionized water and absolute ethyl alcohol several times followed by a drying step at 450 °C for 2 h.

Preparation of $\text{TiO}_2/\text{Ag}/\text{Ag}_3\text{PO}_4$ NRAs. Firstly, silver nitrate (AgNO_3) was dissolved in deionized water containing 20% absolute ethyl alcohol to form AgNO_3 precursor solution with a concentration of 0.002 M⁷. Then the TiO_2 NRAs were immersed in the above solution, and illuminated by a 300 W Xe lamp for 5 minutes. Then the TiO_2/Ag heterostructured nanorod arrays (denoted as TiO_2/Ag NRAs) were rinsed with deionized water and absolute ethyl alcohol several times and dried at 60 °C in air. Secondly, the TiO_2/Ag NRAs were immersed in the above AgNO_3 solution for 40 min. Then transfer it to the NaH_2PO_4 solution for 15 min. The achieved product was then rinsed with deionized water.

Characterization and Evaluation of photocatalytic and photoelectrochemical performance. The morphology and the crystalline structure of the products were examined by scanning electron microscope (SEM, JSM-6480, JEOL) and X-ray diffraction analysis (Lab-XRD-6000, Japan). The photocatalytic performance of the samples were evaluated by using the degradation of RhB (10 mg/L, 50 mL) as the probe reaction under visible light irradiation. The photoelectrochemical measurements were performed in a typical three-electrode system with a piece of Pt foil (1×2 cm) and a saturated calomel electrode (SCE) as counter and reference electrodes, respectively. And the samples were employed to be the working electrodes. The whole photoelectrochemical tests were carried out in an electrolyte medium containing 0.5 M Na_2SO_4 at room temperature, and the experiment data were recorded by an electrochemical workstation (CHI660D).

Results and Discussion

SEM Analysis. The morphology of the TiO_2 NRAs could be observed in Fig.1A and B. The uniform TiO_2 NRAs are vertically aligned into well-defined arrays. Their diameter is from 300 nm to 400 nm. The cross-sectional SEM image (inset in Fig.1A) reveals that the TiO_2 NRAs have lengths of ca. 3 μm . However, when TiO_2 NRAs were dipped into an aqueous AgNO_3 solution, as shown in Fig.1C and D, uniform Ag nanoparticles with a diameter of approximately 150 nm have been successfully grafted on the top regions of TiO_2 NRAs. Moreover, Fig.1E and F show that the SEM images of the $\text{TiO}_2/\text{Ag}/\text{Ag}_3\text{PO}_4$ NRAs. The uniform Ag_3PO_4 have been successfully deposited around the top regions of TiO_2/Ag NRAs, which indicates that we obtained the heterostructured nanorod arrays as what we have expected.

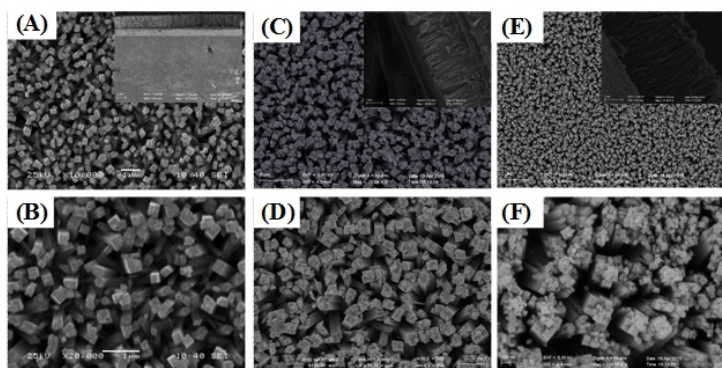


Fig. 1 Top-view SEM images of TiO_2 (A and B), TiO_2/Ag (C and D) and $\text{TiO}_2/\text{Ag}/\text{Ag}_3\text{PO}_4$ NRAs (E and F); the insets show the cross-sectional images of TiO_2 (A), TiO_2/Ag (C) and $\text{TiO}_2/\text{Ag}/\text{Ag}_3\text{PO}_4$ NRAs (E), respectively.

XRD Analysis. The crystalline structure of the samples have been systematically investigated by X-ray diffraction analysis (XRD), and the results are shown in Fig.2. The weak peaks at $2\theta=25.685^\circ$ can be attributed to the standard diffraction of tetragonal anatase TiO_2 and the peaks at $2\theta=27.30^\circ$, $2\theta=35.86^\circ$, $2\theta=40.99^\circ$, $2\theta=54.01^\circ$, $2\theta=62.60^\circ$ indexed to the standard diffraction of tetragonal rutile TiO_2 . Above results show that the as-prepared TiO_2 NRAs are mixed phase of anatase and rutile. The peaks of TiO_2/Ag and $\text{TiO}_2/\text{Ag}/\text{Ag}_3\text{PO}_4$ NRAs at $2\theta=38.26^\circ$ and $2\theta=64.71^\circ$ are assigned to the standard diffraction of Ag (JCPDS-87-0719). And the peaks of $\text{TiO}_2/\text{Ag}/\text{Ag}_3\text{PO}_4$ NRAs at $2\theta=36.49^\circ$

can be indexed to the (211) plane of the standard diffraction of Ag_3PO_4 (JCPDS-71-1836). These results confirm that $\text{Ag}/\text{Ag}_3\text{PO}_4$ nanoparticles have been successfully combined with the TiO_2 NRAs.

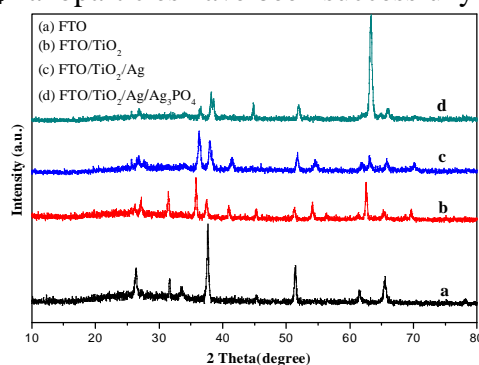


Fig. 2 XRD patterns of FTO, TiO_2 NRAs, TiO_2/Ag and $\text{TiO}_2/\text{Ag}/\text{Ag}_3\text{PO}_4$ NRAs, respectively.

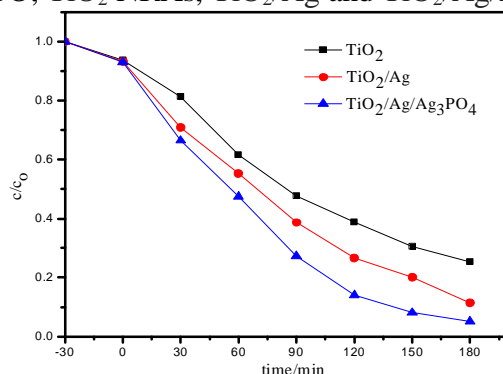


Fig. 3 Photodegradation curve of RhB by TiO_2 , TiO_2/Ag and $\text{TiO}_2/\text{Ag}/\text{Ag}_3\text{PO}_4$ NRAs.

In order to study the photocatalytic activity of the samples, RhB as the target pollutants was used to test the catalytic activity of the hybrid in the process of degradation of pollutants in water under visible light, and the results are shown in Fig.3. To discount the adsorption effect of catalyst on the RhB dye molecules in the dark, the suspension was stirred for 30 min in the dark to achieve the adsorption and desorption equilibration before the photocatalytic activity test. However, $\text{TiO}_2/\text{Ag}/\text{Ag}_3\text{PO}_4$ NRAs show a much higher photocatalytic performance on the degradation of RhB. The photocatalytic efficiency of $\text{TiO}_2/\text{Ag}/\text{Ag}_3\text{PO}_4$ NRAs within 3 hours can reach about 94.5 %. Under the same conditions, TiO_2 NRAs is only 74.8%.

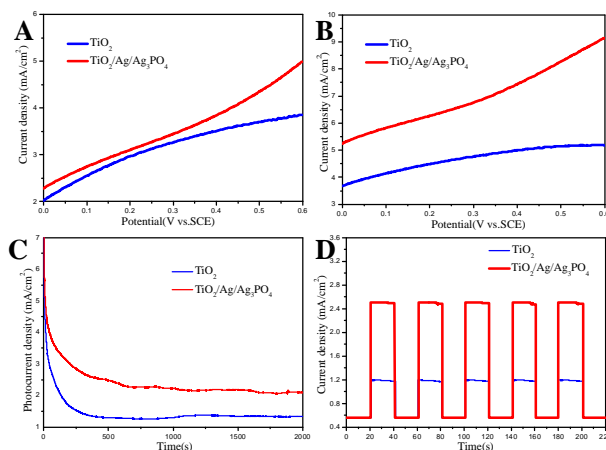


Fig. 4 Linear sweep voltammograms of the TiO_2 and $\text{TiO}_2/\text{Ag}/\text{Ag}_3\text{PO}_4$ NRAs in the dark (A) and under illumination (B); Working lifetime of $\text{TiO}_2/\text{Ag}/\text{Ag}_3\text{PO}_4$ and TiO_2 NRAs under illumination with an applied voltage of +0.2 V(C). Amperometric I-t curves of the TiO_2 and $\text{TiO}_2/\text{Ag}/\text{Ag}_3\text{PO}_4$ NRAs at an applied voltage of +0.2 V with 20 s light on/off cycles(D).

Photoelectrochemical Measurements. The photoelectrochemical performances of the samples were carried out under visible light illumination. Fig.4A and B show the linear sweep voltammograms

of the samples in the dark and under irradiation, respectively. It can be clearly seen that the dark current densities are quite low compared with the photocurrent densities. Compared with the TiO_2 NRAs, the photocurrent densities of the $\text{TiO}_2/\text{Ag}/\text{Ag}_3\text{PO}_4$ NRAs have been greatly enhanced under the visible illumination. In addition, the working lifetime of the samples were shown in Fig.4C. The photocurrent densities of the samples all experience rapidly decline in the initial stage. After 800 s, their photocurrent density are reduced to about $1.30 \text{ mA}\cdot\text{cm}^{-2}$ and $2.50 \text{ mA}\cdot\text{cm}^{-2}$, respectively. Then the photocurrent density tends to be gentle with the continuous extension of the illumination time. Furthermore, as shown in Fig.4D, their $I-t$ curves at applied voltage of +0.2V further demonstrate that the photocurrent density has been greatly improved when the TiO_2 NRAs were grafted with $\text{Ag}/\text{Ag}_3\text{PO}_4$. The maximum photocurrent density of the $\text{TiO}_2/\text{Ag}/\text{Ag}_3\text{PO}_4$ NRAs can achieve $2.60 \text{ mA}\cdot\text{cm}^{-2}$, which is much higher than $1.20 \text{ mA}\cdot\text{cm}^{-2}$ of the pure TiO_2 NRAs.

Conclusions

In summary, we have demonstrated a facile and efficient strategy for the fabrication of $\text{TiO}_2/\text{Ag}/\text{Ag}_3\text{PO}_4$ NRAs. The modification of $\text{Ag}/\text{Ag}_3\text{PO}_4$ nanoparticles onto TiO_2 NRAs could facilitate a more effective separation of photoexcited electron-hole pairs and help to extend the absorption spectrum of the TiO_2 NRAs significantly into visible region, thus boost up the photoelectrochemical and photocatalytic performances. The materials based on FTO conductive glass are easier to recycle compared with powders.⁸ Consequently, the $\text{TiO}_2/\text{Ag}/\text{Ag}_3\text{PO}_4$ NRAs in this work might be used in a wide range of applications, such as photocatalysis, electrode sensors and solar cells. It is now being explored that this effective synthetic route would also be extended to fabricate other photoelectric materials to enhance their properties and potential applications.

Acknowledgements

This work was financially supported by the National Natural Science Foundation of China (No.51208233) and the Natural Science Foundation of Jiangsu Province, China (No.BK2012699).

References

- [1] Z. H. Xu and J. G. Yu, *Nanoscale* 3, 3138 (2011).
- [2] J. Zhang, J. H. Bang, C. C. Tang and P. V. Kamat, *ACS. Nano.* 4, 387 (2010).
- [3] M. R. Hoffmann, S. T. Martin, W. Y. Choi and D. W. Bahnemann, *Chem. Rev.* 95, 69 (1995).
- [4] T. Berger, M. Sterrer, O. Diwald, E. Knozinger, D. Panayotov and T. L. Thompson, *J. Phys. Chem. B* 109, 6061 (2005).
- [5] W. Teng, X. Y. Li, Q. D. Zhao and G. H. Chen, *J. Mater. Chem. A* 1, 9060 (2013).
- [6] T. H. T. Vu, H. T. Au, L. T. Tran, T. M. T. Nguyen, T. T. T. Tran, M. T. Pham, M. H. Do and D. L. Nguyen, *J. Mater. Sci.* 49, 5617 (2014).
- [7] T. Wang, Z. B. Jiao, T. Chen, Y. W. Li, W. Ren, S. L. Lin, G. X. Lu, J. H. Ye and Y. P. Bi, *Nanoscale* 5, 7552 (2013).
- [8] I. Tacchini, E. Terrado, A. Anson and M. T. Martinez, *J. Mater. Sci.* 46, 2097 (2011).